AIMS Energy, 13(4): 938–961.
DOI: 10.3934/energy.2025035
Received: 05 June 2025
Revised: 27 July 2025
Accepted: 08 August 2025
Published: 19 August 2025

https://www.aimspress.com/journal/energy

Research article

Scenario-based optimization of standalone microgrids using PSO: comparative assessment of hybrid configurations for off-grid electrification in Unguja Island

Fathia Jombi Kheir[1,*], Soichiro Ueda[1], Takuma Ishibashi[1], Mitsunaga Kinjo[1], Issoufou Tahirou Halidou [1], Masahiro Furukakoi[2] and Tomonobu Senjyu[1]

[1] Faculty of Engineering, University of the Ryukyus, Okinawa 903-0213 Japan

[2] Sanyo-Onoda City University, Yamaguchi, 756-0884, Japan

* **Correspondence:** Email: k238488@cs.u-ryukyu.ac.jp; Tel: +818043146517.

Abstract: Access to a sustainable and reliable power supply has been a major struggle for most remote and rural communities, particularly on Islands. This is largely due to the uncertainties and vulnerabilities imposed by grid extension and electricity importation. This study employed a Particle Swarm Optimization (PSO) approach to assess the performance of three off-grid microgrid configurations: PV/BESS, PV/Wind/BESS, and PV/BESS/DG for electrifying a village in the northern region of Unguja Island. The effective sizing was conducted using real-time and site-specific meteorological and demand data. The primary goal was to minimize the Levelized Cost of Energy (LCOE) while satisfying the reliability constraint defined as the Loss of Power Supply Probability (LPSP), below 4%. The results demonstrated that the PV/Wind/BESS configuration exhibited the lowest LCOE at \$0.014/kWh; 13.6% and 46.2% lower than the PV/BESS and PV/BESS/DG configurations, respectively. Although the PV/BESS/DG scenario demonstrated greater reliability compared to other cases, it incurred the highest LCOE over the project lifetime, which was attributed to volatile fuel prices and elevated operational costs. Furthermore, the sensitivity analysis highlighted the substantial influence of life-cycle costs, including component replacement and operational maintenance costs, on the long-term economic viability of the proposed microgrid configurations. These insights offer valuable strategic guidance for energy policymakers aiming to enhance energy security and autonomy in rural and underserved communities.

Keywords: Off-grid Microgrids; Levelized Cost of Energy; Loss of Power probability; PSO; PV system; Wind energy System; DG system; Zanzibar; CO_2 emissions

1. Introduction

1.1. Motivation

Despite significant technological progress achieved throughout the twentieth century, access to stable, reliable, and sustainable electricity remains a critical challenge for approximately 1.3 billion people around the world, particularly on islands and in remote areas [1]. In Africa, as reported from the last Mission 300 Africa Energy Summit [2], more than 600 million people lack access to stable and reliable electricity. This restricts access to quality education and health services, slows economic development, and exacerbates discrepancies around the world. In addition, more than 70% of the primary source of energy in Africa is biomass, sourced from burning trees, leading to increased carbon emissions and environmental degradation, while ironically, Sub-Saharan Africa has a vast untapped potential for renewable energy sources [3].

As the global energy consumption continues to soar, the reliance on fossil fuels raises critical concerns about long-term energy security and environmental conservation. Despite remaining a dominant conventional energy source, the transition to a more sustainable alternative is essential for long-term sustainability, energy security, and environmental benefits [4]. Currently, the world is aligning with the integration of renewable energy sources, which offer a promising solution by harnessing clean, naturally replenishing, and abundant sources such as solar, wind, geothermal, biomass, and hydro sources [5]. Technological advancements coupled with supportive policy measures, such as the feed-in tariffs, have accelerated the cost decline of renewable components, particularly solar panels, which have further enhanced the economic attractiveness of renewable projects. The global cost of solar PV electricity decreased by approximately 41% between 2015–2016 and 2019–2020, indicating the growing deployment of solar energy projects throughout the world [6].

Unguja Island in Figure 1, located 25–50 km off the East African Coast in the Indian Ocean, is a great example of these power challenges. The island is popular for its cinematic beauty and thriving tourism sector. Unfortunately, the Island relies entirely on the electricity imported from the Tanzania mainland via submarine cables. Unguja Island imports approximately 130 MW via a 45 MW cable, which is now degraded to 30 MW, and via a new 100 MW submarine cable. Moreover, the island has idle diesel generators, which were installed to serve the load demand before the commissioning of the new cable. This dependency has imposed several power insecurities on the island, especially as the Island's demand continues to surge, driven by the rapid pace of investments across sectors, including tourism. The Island frequently experiences power outages caused by the existing infrastructure operating at its near full capacity, with the newer cable already utilized at 93.3% [7].

The North Region of Unguja is a prominent tourist destination and hosts large hotels that consume a significant portion of the region's electricity. Persistent technical issues in the island's grid have pushed many of these hotels to install their private solar mini-grids and rely on diesel generators at night. However, this operation is costly and has caused inconveniences for many investors [8]. To address this, the government is currently putting efforts into installing renewable plants such as Solar PV and Battery Energy Storage Systems as a part of the Zanzibar Energy Sector Transformation and Access project supported by the World Bank to enhance its energy security [9]. Moreover, emphasis on the adoption of renewable and modern energy sources has been a hot topic in the country. Several feasibility studies have been conducted to research the viability of renewable projects in Zanzibar.

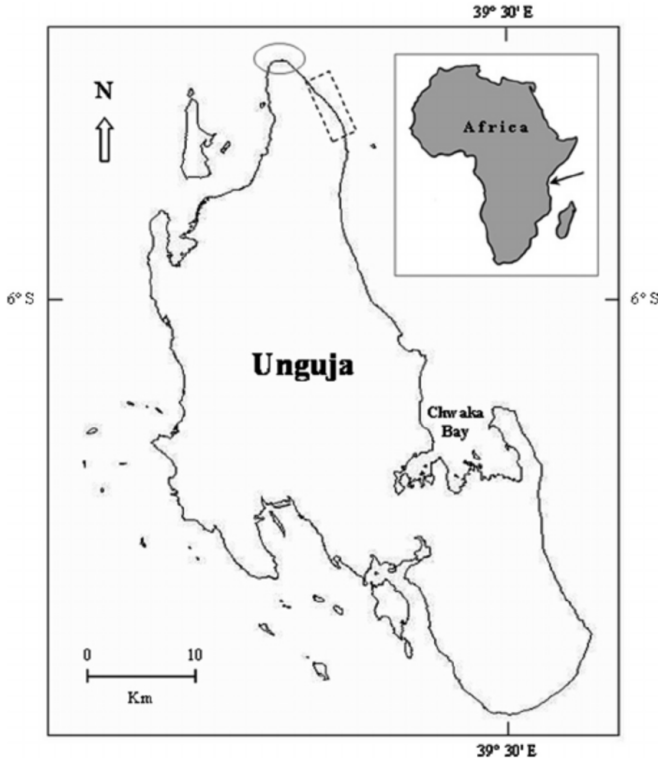

Figure 1. A map showing the geographical location of the Unguja Island along the East African Coast.

1.2. Literature review

Although the integration of renewable energy into the power system is crucial for achieving a sustainable power supply and lower carbon emissions, the inherently intermittent nature of renewable sources poses a major challenge to ensuring consistent and reliable power generation [10]. To address this, several researches have compared the performance of utilizing a single renewable source, such as wind or solar, to the hybrid systems, which integrate multiple energy sources such as photovoltaic/wind, photovoltaic/wind/biomass, and photovoltaic/wind/diesel generators often supported by the inclusion of battery energy storage systems (BESS). These researches have demonstrated that hybrid systems are more reliable and cost-effective than single energy sources. The reliance on single energy sources results in component over-sizing, leading to increased capital investment and operational cost of the system [11]. Furthermore, the sustainability of the energy transition lies not only in the deployment of modern energy sources or advanced clean technologies, but it should also promote the cost-effectiveness of the energy solutions [12].

A critical aspect of microgrid design lies in the proper sizing of its components to meet a given load demand. To address the complex sizing of microgrids, various simulation-based tools, deterministic models, and metaheuristic algorithms have been developed and presented in the literature reviews of many studies. According to [13], tools such as HOMER, RETScreen, and PVSyst are widely used in microgrid sizing; however, these platforms offer limited flexibility for the user to modify the underlying equations or customize the algorithms. In [14], a comprehensive review and analysis of 19 software tools, including HOMER, RETScreen, HYBRID2, and IHOGA, was conducted, where

HOMER was identified as mostly user-friendly and a widely used tool. Particle Swarm Optimizer (PSO) and HOMER tools were utilized in [15] to optimize and perform a sensitivity analysis for rural electrification in Algeria using a PV/diesel/battery hybrid energy system. Compared to HOMER, the results from the PSO-based approach proved to be more cost-effective with higher renewable penetration. A comparative analysis of two meta-heuristic methods, PSO and Genetic Algorithm (GA), was performed by [16] for the sizing problem of hybrid energy systems. Key economic indicators such as the Net Present Cost (NPC), Cost of Energy (COE), and overall generation cost (GC) were used in the evaluation. The findings indicated that the PSO approach outperformed GA in optimizing microgrid configurations.

In [17], mixed integer linear programming (MILP) was implemented to calculate the optimal size of a hybrid wind-photovoltaic power plant in an industrial area. Considering load and seasonal variability, optimization was performed separately for each month of the year. The methodology was tested to analyze an industrial plant in the Rome area. The authors in [18] employed a Genetic Algorithm (GA) in optimal sizing for the stand-alone microgrid problem comprising solar PV, wind turbines, battery energy storage system (BESS), and diesel generators. The considered optimization objectives included minimizing the system life-cycle cost, maximizing renewable penetration, and reducing emissions. In [19], the latest metaheuristic algorithm, Grasshopper Optimization Algorithm (GOA), integrated with a robust Energy Management Scheme (EMS), was utilized and compared with Particle Swarm Optimization (PSO) and CuckooSearch (CS) optimization algorithms in sizing an autonomous hybrid stand-alone microgrid for five residential units in Nigeria. Moreover, a sensitivity analysis was performed to analyze the impact of variation in sensitive inputs such as the fuel price, solar radiation, wind speed, and the battery state of charge (SOC) setpoint on the cost of energy production (COE). A Modified Firefly Algorithm (MFA) was applied in [20] for the optimal sizing of stand-alone operating solar microgrids; the methodology confirmed to have an improved convergence speed and solution quality. Further, the suitability of the methodology was proved through a case study.

1.3. Contribution and paper organization

Ensuring a consistent and sufficient power supply is crucial in remote areas and islands, where the reliance on generators and electricity imports is costly and vulnerable to disruptions. In response to the challenge facing Unguja Island, this paper proposes three microgrid scenarios comprising PV/BESS, PV/Wind/BESS, and PV/BESS/DG. Each scenario is sized using Particle Swarm Optimization (PSO) to minimize the Levelized Cost of Energy (LCOE) over the project lifetime while satisfying reliability constraints. The key contributions of this paper are highlighted as follows:

1. To the best of the author's knowledge, this paper contributes to the research gap on hybrid microgrid research in Unguja Island. At present, many feasibility studies predominantly entail the system with a single renewable source, such as solar PV or wind, supported with batteries. However, the uniqueness of this paper lies in comparing the performance of relying on single-renewable energy sources with the integrated renewable systems, in assessing the cost-effectiveness and reliability for electricity generation on the island.
2. To the best of the author's knowledge, this paper studies the inclusion of diesel generators in electrifying a remote village in the North of Unguja. While ongoing research focuses on renewable sources, this paper revisits the potential of employing the idle diesel generators as

part of the hybrid microgrid solution. By assessing its performance on compensating for energy shortages, and increasing the reliability of continuous electricity supply in the region.

3. In addition, a comprehensive sensitivity analysis is conducted to examine the impacts of individual components' operation and maintenance, as well as replacement cost, which are highly influenced by the inflation rates, discount rates, and change in the fuel prices on the Levelized Cost of Energy (LCOE) of each case scenario.

The rest of the paper is organized as follows: Section 2 outlines the data sources and describes the methodological framework of the proposed optimization approach. Section 3 presents the results and discusses the simulation results of each case scenario, including a sensitivity analysis. Finally, Section 4, summarizes the key findings and offers concluding remarks.

2. Materials and methods

This paper designs and evaluates the best microgrid configuration by comparing three microgrid designs: PV/BESS, PV/Wind/BESS, and PV/BESS/DG systems as shown in Figure 2. The evaluation focuses on minimizing the Levelized Cost of Energy (LCOE) of the system while constraining the system's reliability. The simulation is performed using a Particle Swarm Optimizer (PSO). Data used in this study include annual hour load demand data of a village in the northern region of Unguja for the year 2023. The data are collected from Zanzibar Electricity Corporation (ZECO), which is the main electricity distribution company owned by the Revolutionary Government of Zanzibar. Meteorological data, including solar irradiation, ambient temperature, and wind speed, are collected from the NASA website [21].

2.1. Microgrid modeling

2.1.1. Solar PV model

The power output from the solar panels can be derived from the formula below [22]:

$$P_{\mathrm{PV}} = Y_{\mathrm{PV}} \times f_{\mathrm{PV}} \times \frac{I_T}{1000} \times \{1 + \alpha'(T_C - T_S)\} \tag{2.1}$$

where

- P_{PV} depicts the power output of the solar PV module,
- Y_{PV} indicates the power of a single PV module,
- f_{PV} stands for the derating factor (to accommodate dust loss and ambient temperature effects on the PV module),
- I_T is the total solar radiation incident on the PV module (W/m^2),
- α' represents the temperature index (%/°C),
- T_C denotes the cell temperature, and
- T_S represents the temperature of the cell at standard test conditions (STC).

The cell temperature is given by [22]:

$$T_C(t) = T_a(t) + \left(\frac{\mathrm{NOCT} - 20}{0.8}\right) \cdot \frac{I_T}{I_S} \tag{2.2}$$

where:

- $T_C(t)$ shows the cell temperature (°C),
- $T_a(t)$ shows the ambient temperature (°C),
- I_S stands for the radiation at STC, and
- NOCT stands for the nominal operating cell temperature (°C).

2.1.2. Wind system modeling

Power output from wind is given by the following equation [1]:

$$P_{\mathrm{WT}}(t) = \begin{cases} 0, & v(t) \le v_{\text{cut-in}} \text{ or } v(t) \ge v_{\text{cut-out}} \\ P_r\left(\frac{v(t)^3 - v_{\text{cut-in}}^3}{v_r^3 - v_{\text{cut-in}}^3}\right), & v_{\text{cut-in}} < v(t) < v_r \\ P_r, & v_r \le v(t) < v_{\text{cut-out}} \end{cases} \tag{2.3}$$

where:

- P_r: Rated power,
- v_r: Rated velocity,
- $v_{\text{cut-in}}$: Cut-in velocity,
- $v_{\text{cut-out}}$: Cut-out velocity.

2.1.3. Battery energy storage modeling

The battery energy storage is designed to cover the periods of deficit and excess by discharging and charging during surplus. However, the battery is constrained to stay within the state of charge limits (SOC) to avoid battery overcharge and discharge [23].

$$\mathrm{SOC}_{\min} < \mathrm{SOC}(t) < \mathrm{SOC}_{\max} \tag{2.4}$$

- Charging: When there is excess power, the batteries are charged, and the charged energy is given by [24]:

$$E_{CH}(t) = \left(P_{RES}(t) - \left(\frac{P_L(t)}{\eta_{inv}}\right)\right) \times \Delta t \times \eta_{ch} \tag{2.5}$$

Because of charging, the State of Charge is incremented by [24]:

$$SOC(t) = SOC(t-1)(1-\sigma) + E_{CH}(t) \tag{2.6}$$

- Discharging: When there is an energy deficit, the battery discharges to cover for the shortage that is unmet by the renewables. The discharge equation is given by [24]:

$$E_{disch}(t) = \left(\frac{P_L(t)}{\eta_{inv}} - P_{RES}(t)\right) \times \Delta t \times \eta_{disch} \tag{2.7}$$

Because of the discharge, now the State of Charge is decreased by [24]:

$$SOC(t) = SOC(t-1) \times (1-\sigma) - E_{disch}(t) \tag{2.8}$$

2.1.4. Diesel generator modeling

Diesel generators are mostly recommended for off-grid microgrids to supply power in times when renewables cannot meet the demand [25]. However, the diesel generator system is associated with a lot of costs, which include higher operation and maintenance costs as well as higher fuel prices and environmental constraints [26]. The quantity of fuel consumed by the generator(L/h) is given by equation [27]:

$$F = (F_{0,\mathrm{DG}} \times Y_{\mathrm{DG}}) + (F_{1,\mathrm{DG}} \times P_{\mathrm{DG}}) \tag{2.9}$$

- F is the fuel consumed by the diesel generator (DG) (L/h).
- $F_{0,\mathrm{DG}}$ is the fuel coefficient of intercept in Fuel curve (L/kWh).
- Y_{DG} is the DG rated capacity (kW).
- $F_{1,\mathrm{DG}}$ is the slope of the curve (L/kWh).
- P_{DG} is the power output of the diesel generator (kW).

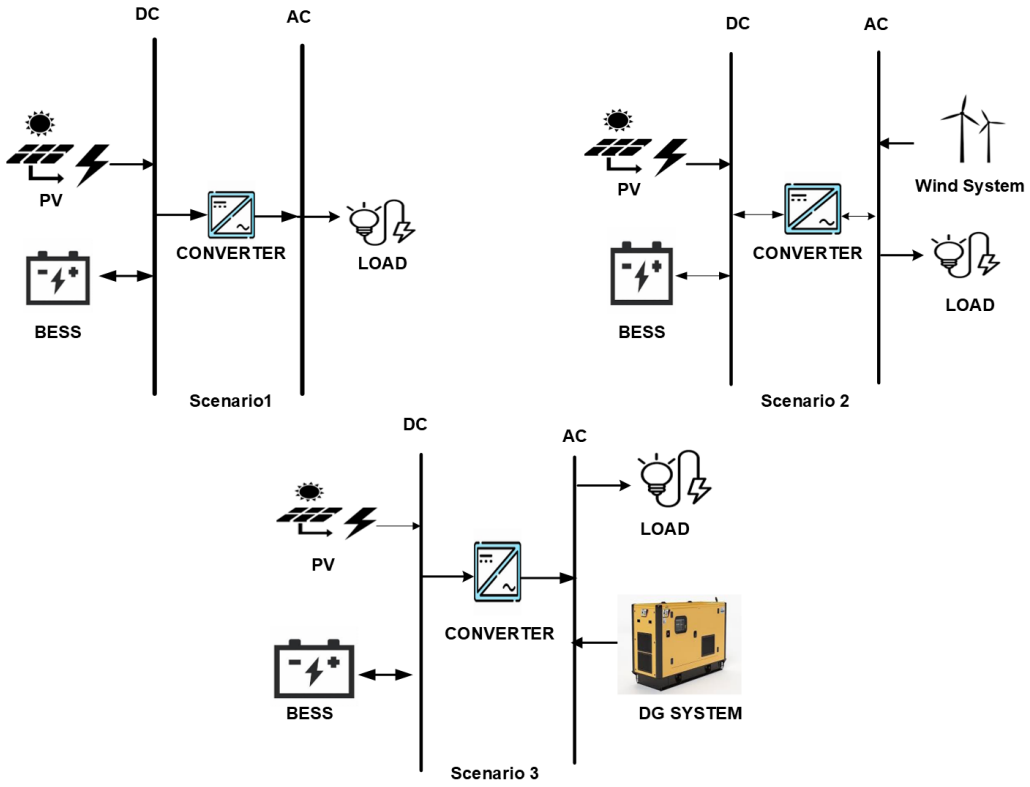

Figure 2. Optimized case scenario configurations for powering a village in the Northern Region of Unguja Island.

2.2. Energy balance

In standalone hybrid microgrid operations, energy balance is vital to ensure a reliable and continuous power supply. When the power generated from renewable sources (solar PV or wind) is higher than the load demand, the excess energy is directed to the battery energy storage for charging. Under these conditions, the flow of energy is given by:

$$P_L(t) \times \Delta t + E_{\text{CH}}(t) \times \eta_{\text{conv}} = P_{\text{WT}}(t) \times \Delta t + (P_{\text{PV}}(t) \times \Delta t) \times \eta_{\text{conv}} \tag{2.10}$$

However, if the excess energy is greater than the battery storage capacity, the energy is dumped. The dumped energy can be calculated from the following formula:

$$P_{\text{dummy}}(t) \times \Delta t = (P_{\text{WT}}(t) - P_L(t)) \times \Delta t + (P_{\text{PV}}(t) \times \Delta t - E_{\text{CH}}(t)) \times \eta_{\text{conv}} \tag{2.11}$$

Moreover, when the power from the renewable sources cannot meet the load demand, the battery storage systems intervene by discharging the stored power into the Load. At discharge, the flow of energy can be expressed as:

$$P_L(t) \times \Delta t = P_{\text{WT}}(t) \times \Delta t + (P_{\text{PV}} \times \Delta t + E_{disch}(t)) \times \eta_{\text{conv}} \tag{2.12}$$

In a system where the BESS is fully depleted and the diesel generator is available, the power flow is given by:

$$P_L(t) \times \Delta t = P_{\text{DG}}(t) \times \Delta t - (P_{\text{PV}}(t) \times \Delta t + E_{\text{disch}}(t)) \times \eta_{\text{conv}} \tag{2.13}$$

2.3. Techno-economic viability vs. reliability

The objective function in this paper is the minimization of the LCOE; the PSO is designed to select the best microgrid that gives the lowest LCOE; while the Loss of Power Supply probability (LPSP) was constrained to be not higher than 4%.

2.3.1. Levelized Cost of Energy

The Levelized Cost of Energy (LCOE), also known as the Levelized Cost of Electricity, is a crucial financial parameter used to determine the feasibility of an energy investment; it represents the lifetime cost of generating a unit of energy [28]. A higher LCOE indicates that it is expensive to produce a unit of energy using that generation system. The LCOE is calculated by dividing the total cost of building and operating a power plant throughout the lifetime of the project by the total power produced within that lifetime [29]. LCOE is given by [30]:

$$\text{LCOE} = \frac{\text{NPC} \cdot \text{CRF}}{PL_T} \tag{2.14}$$

where PL_T is the Total Energy produced.

The Net present cost (NPC) of a system is a summation of the present value cost of each component in a system, including capital investment, operation, and maintenance cost throughout a project lifetime, minus the present value of the total revenue obtained throughout the project period [31]. The NPC of the system is given by [30]:

$$\text{NPC} = C_{\text{ap}} + C_{\text{om}} + C_{\text{fc}} - C_{\text{sal}} \tag{2.15}$$

where C_{ap} is the capital cost, C_{om} is the NPC of operation and maintenance, C_{fc} is the NPC of the fuel cost (if the system includes a diesel generator), and C_{sal} is the NPC of the salvage value of the components.

The Cost recovery factor (CRF) is a financial parameter that converts the present value of costs into a series of equal annual cash flows over the life of the project [32]. It is given by:

$$\text{CRF} = \frac{i(1+i)^y}{(1+i)^y - 1}$$

2.3.2. Loss of power supply probability (LPSP)

LPSP is a reliability metric that measures the probability of the system failing to meet the load demand. The values of LPSP range between 0 and 1, where 0 indicates that the system meets the demand all the time, while 1 indicates that demand is never met [33]. The LPSP is defined by the ratio of power shortage to the total load demand [34]:

$$\text{LPSP} = \frac{\sum_{t=1}^{8760} Shortage(t)}{\sum_{t=1}^{8760} P_{L(t)}} \tag{2.16}$$

To realize a better trade-off between the LCOE and LPSP, for this paper, the LPSP is constrained to be below 0.04.

2.4. Particle swarm optimization (PSO) approach

The PSO approach is a popular tool used in microgrid optimization owing to its simplicity, robustness, and fast computational performance. It is an evolutionary algorithm inspired by the collective social behavior exhibited within a flock of birds or fish schools in locating food and avoiding predators [35]. This approach was first introduced by Kennedy and Eberhart in 1995; based on their observations of how coordinated movements of these animals led to the discovery of near-global optimum solutions.

In the context of microgrid system optimization, PSO offers several advantages over other metaheuristic algorithms, such as Genetic Algorithm (GA), Harmony Search (HS), and Artificial Bee Colony (ABC). PSO exhibits the fastest convergence rate as well as strong global search capabilities, making it well-suited for solving complex optimization problems, such as those associated with hybrid microgrid sizing [36]. Based on these advantages, PSO is selected as the preferred optimization tool in this study.

The PSO approach consists of several initialized N populations known as swarm particles with random positions and velocities. Each swarm particle represents a potential solution and is characterized by its current position. $X_{ij} = (X_{i1}, X_{i2}, \ldots, X_{iM})$ and velocity $V_{ij} = (V_{i1}, V_{i2}, \ldots, V_{iM})$, The index is in the range of

$$i \in \{1, 2, \ldots, N\}, \quad j \in \{1, 2, \ldots, M\}$$

within search space M. The algorithm iteratively updates these attributes, navigating the swarm toward the near-global optimum solution [37][38].

In this study, an adaptive stopping criterion is implemented. The algorithm is set to stop when there is no improvement in the global best fitness value (Gbest). To ensure this, a threshold value of $\epsilon = 10^{-5}$ was chosen for consecutive iterations of $K = 50$. In addition, a maximum of 500 iterations is set to prevent unnecessary computations when the solution is not converging. The PSO workflow for this paper is presented in Figure 3. The algorithm is implemented in MATLAB and tested across all microgrid scenarios under identical environmental and economic constraints. The key input parameters to the optimization algorithm are presented in Table 1.

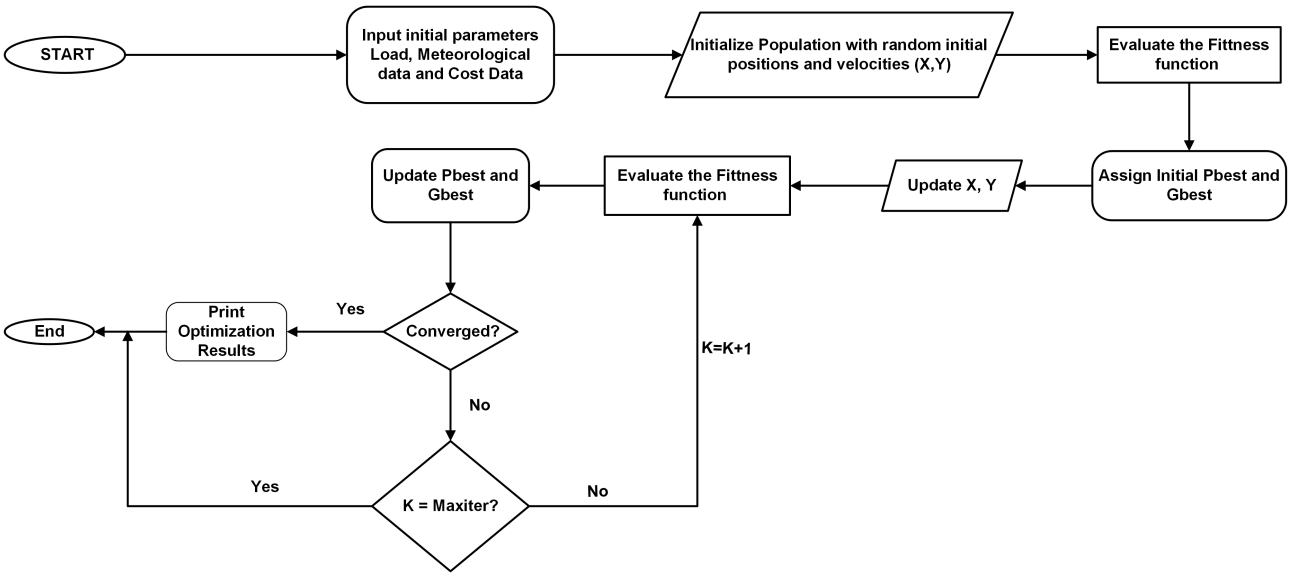

Figure 3. PSO work flow for the sizing problem of the microgrid scenarios.

Table 1. Key input parameters.

Parameter	Value	Reference
Interest Rate *(i)*	6%	[39]
Project Lifetime *(y)*	25 years	
PV panels efficiency	19.8%	[40]
PV panels lifetime	25 years	[40]
PV panels capital cost ($/kW)	500	[41]
BESS capital cost ($/kW)	400	[41]
BESS O&M cost ($/kW)	8	[42]
BESS Replacement cost ($/kW)	350	[41]
BESS lifetime	10 years	[41]
Wind energy system cost ($/kW)	1170	[43]
Wind O&M cost ($/kW/year)	43	[44]
Wind Replacement cost ($/kW)	75% of initial cost	[45]
Wind energy system lifetime	20 years	
DG capital cost ($/kW)	0	
DG O&M cost ($/kW/year)	5	[41]
DG Replacement cost ($/kW AC)	350	[41]
DG rated capacity	800 kW	

3. Results and discussion

This paper aims to determine the best microgrid configuration for standalone operation for a village in the north region of Unguja Island that can operate at the lowest cost and ensure the reliability of energy. Different scenarios are simulated to analyze their performance in ensuring that demand is served at minimum cost. The results are simulated using the hourly load demand of the region.

3.1. Load demand

Figure 4 presents the monthly average load demand of a village in the north region of Unguja for the year 2023. The figure demonstrates a seasonal variation in energy consumption. A continuous increase in the energy demand is observed from November to March, coinciding with the summer season in Unguja. This season is characterized by having a sustainable influx of tourists coming from snowy regions, which in turn heightens the electricity demands in hotels and other hospitality sectors. Furthermore, this time frame overlaps with the end and the beginning of the new year, implying a holiday season; hence, many hotels experience a peak occupancy. This situation contributes to power consumption surges as observed in Figure 5, which is the load demand profile for December.

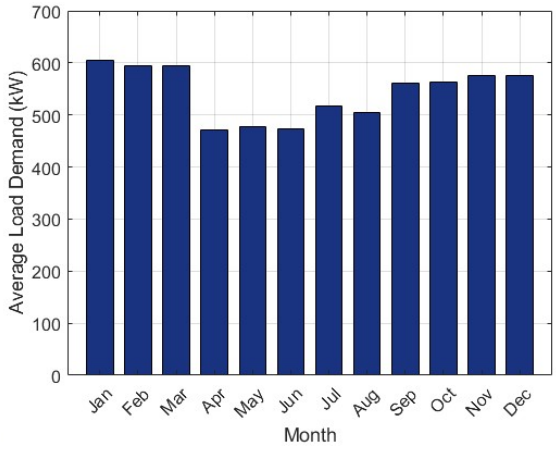

Figure 4. Monthly average power demand profile for a village located in the North Region of Unguja Island.

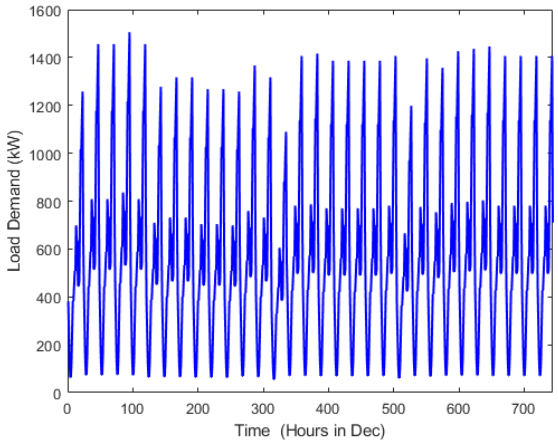

Figure 5. December load demand profile, representing the summer season.

In contrast, a decline is observed from April through June, attributed to the heavy rain season, with a reduction in tourism activities. During this time, many big hotels temporarily close, and some operate at lower capacity, reducing the overall village energy consumption. However, at the beginning

of July, an increase in demand is observed, which is characterized to be the coldest month in Unguja caused by high winds. The rise in power demand is mainly associated with the greater utilization of heat appliances. Additionally, July hosted several big festivals in 2023, which further enhanced demand surges. Figure 6 shows the monthly power demand for July, indicating the winter season.

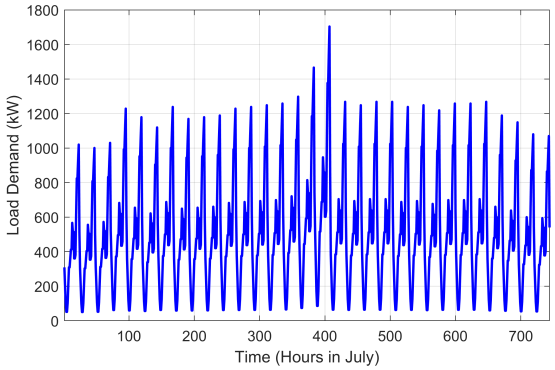

Figure 6. July load demand profile, representing the winter season.

3.2. Meteorological data

Meteorological data that include solar irradiation, ambient temperature, and wind speed data are collected from the NASA climate database. The data shows that the average solar irradiation in the North region of Unguja is 0.216 kW/m². The region has an average wind speed of 6.22 m/s, with a maximum wind speed of 22.71 m/s observed in July. Figure 7 shows the solar irradiation, ambient temperature, and wind speed profile for the day with the maximum solar irradiation in the year 2023.

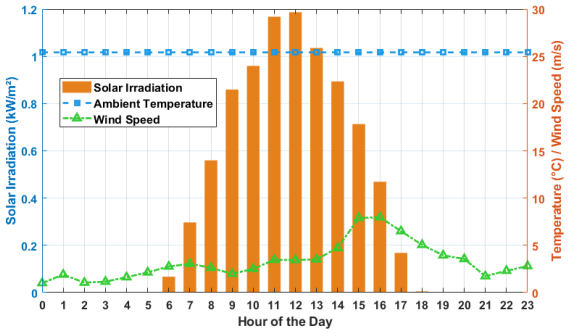

Figure 7. Solar irradiation, ambient temperature, and wind speed profiles, representing a day with maximum solar irradiation in the year 2023.

3.3. PSO simulation results

Three scenarios of microgrid configurations are simulated: PV/BESS, PV/Wind/BESS, and PV/BESS/DG systems. The goal is to minimize the LCOE while maintaining the loss of power probability to be below 4%. The first scenario is taken as a base case to demonstrate how a single system can affect the reliability of the microgrid as compared to hybrid systems. The purpose of the scenarios is to demonstrate the influence of wind and diesel generator systems on the viability of the microgrid.

3.3.1. 1st Scenario

The findings for the 1st scenario, PV/BESS, reveal that meeting the load demand solely with solar PV and BESS requires a substantial investment, particularly in solar PV capacity. Achieving sufficient power generation for daytime consumption requires a solar PV system size of 14,702.7514 kW. To store the surplus power for covering the load demand during hours of no solar irradiation and insufficient solar PV output, a total of 3238 Battery Energy Storage (BESS) units are needed, resulting in an LCOE of \$0.0162/kWh. Figures 8 and 9 show the power produced from solar PV during the winter and summer seasons, specifically July and December, respectively.

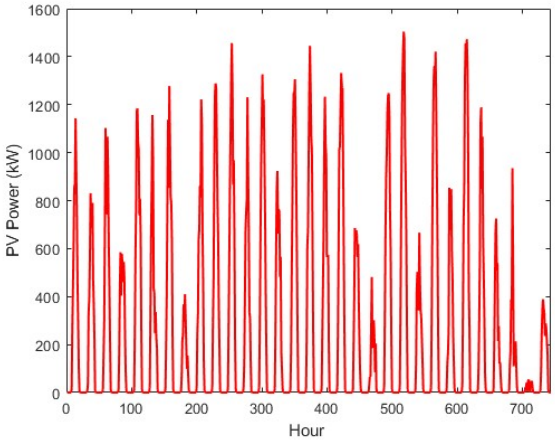

Figure 8. Scenario 1: Solar PV output in July (winter).

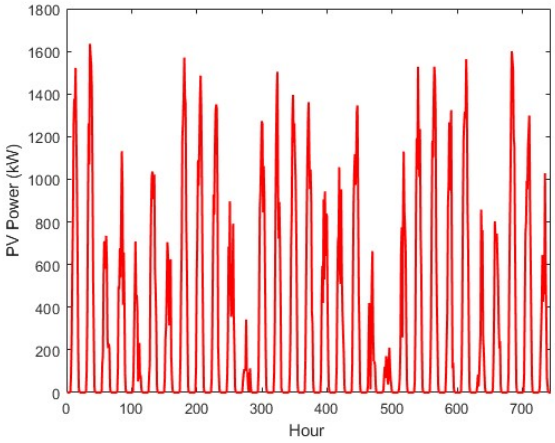

Figure 9. Scenario 1: Solar PV output in December (summer).

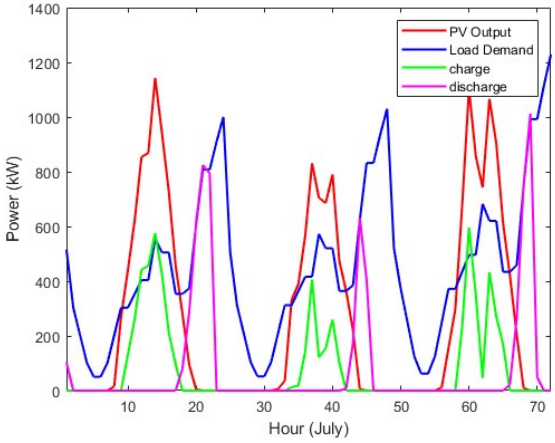

Figure 10. Scenario 1: PV, load and BESS profiles for 3 representative days in July.

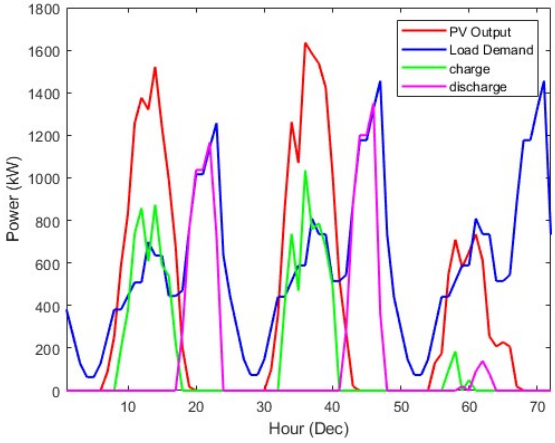

Figure 11. Scenario 1: PV, load and BESS profiles for 3 representative days in December.

Given that the demand is consistently high during these two seasons, a three-day sample was

chosen from each season to demonstrate the PV output, charging, and discharging trend of the system in meeting the load demand. Figures 10 and 11, depict that the solar PV system and BESS exhibit limited reliability, especially under cost-minimization constraints. Both figures reveal that the demand is 90% met during the daytime, and the excess energy is charged to the BESS, only to discharge when there is insufficient or no PV output. However, the BESS discharges, but it is unable to cover all the demand. This is because the acceptable range for the loss of power supply probability is set to be under 4%.

3.3.2. 2nd Scenario

This scenario examines the performance of a hybrid PV/Wind/BESS microgrid system. Relative to Scenario 1, this setup achieves a marked reduction in the required solar PV capacity exceeding 90%. The optimized system components are determined as 1417.38 kW for solar PV, 3069.39 kW for wind power, and 3050 BESS units. The seasonal outputs of renewable generation are shown in Figures 12 and 13, where the variability of wind energy contributes to significant fluctuations in total power production.

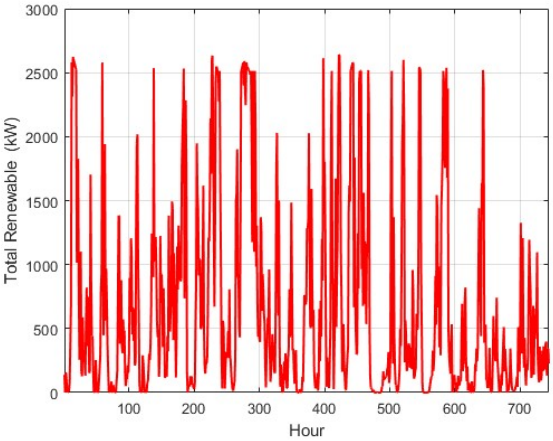

Figure 12. Scenario 2: Total renewable output in July (winter).

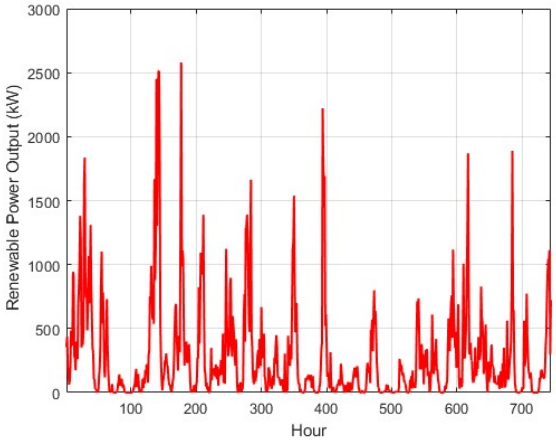

Figure 13. Scenario 2: Total renewable output in December (summer).

To assess the behavior of the system more precisely, a three-day interval is selected for each season, replicating the approach used in Scenario 1. Figure 14 illustrates the winter period, highlighting instances of high renewable generation. During these periods, surplus energy is first directed to battery storage; however, when generation exceeds storage capacity, the excess is curtailed. These occurrences are particularly associated with strong wind periods in July. On days with more moderate conditions, the system successfully meets the demand, with surplus energy efficiently stored. A similar pattern is evident during the summer period, as shown in Figure 15. Intermittent high wind speeds again cause renewable generation to exceed storage limits, resulting in energy dumping; however, the frequency is much lower than in the winter season. In contrast, at certain hours, specifically between hours 48 and 50 and hours 68 and 70, the solar irradiation and wind speed are minimal, and the battery system is fully discharged. These shortages predominantly occur during evening and nighttime hours. This configuration requires low investment compared to the 1st scenario; the inclusion of a wind system

reduces the over-reliance on solar PV, as wind is available beyond the daylight period. The obtained Levelized Cost of Energy (LCOE) is estimated at $0.014/kWh.

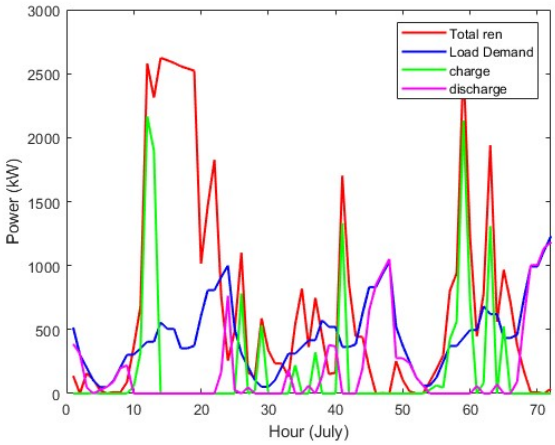

Figure 14. Scenario 2: PV, load, wind & BESS profiles for 3 representative days in July.

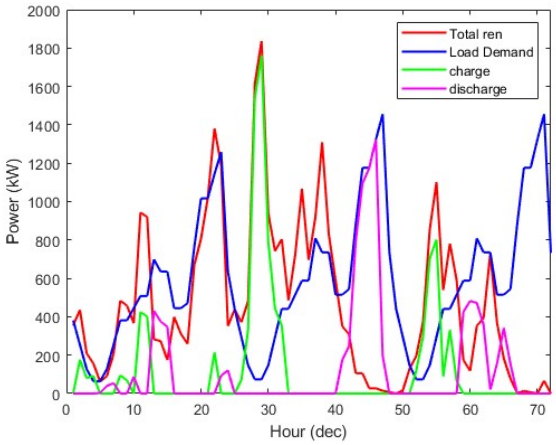

Figure 15. Scenario 2: PV, load, wind & BESS profiles for 3 representative days in December.

3.3.3. 3rd Scenario

For this configuration, a PV/BESS/DG system is optimized with more operational priority given to the solar PV generation and BESS discharging. The diesel generator is programmed to actively operate only when there is minimal or unavailable PV output and the batteries have been fully depleted. This control strategy is intentionally employed to mitigate the environmental impacts of CO_2 emissions and to minimize fuel consumption costs. Figures 16 and 17 depict the diesel generator's performance in compensating for power shortfalls during the winter and summer seasons, respectively. Unlike Scenario 2, in which renewable fluctuations are high, the diesel generator precisely covers the deficit power, enhancing a more stable, nonfluctuating output, which in turn increases the system reliability.

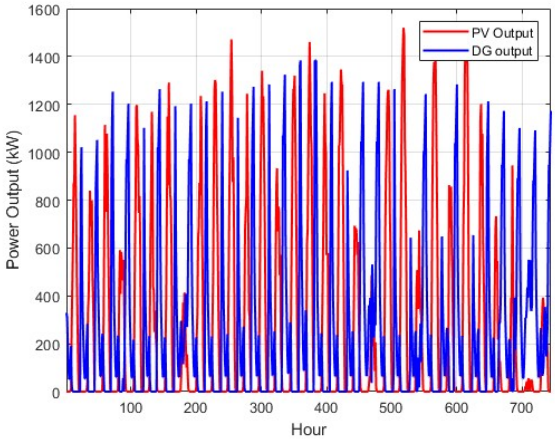

Figure 16. Scenario 3: PV and DG output in July (winter).

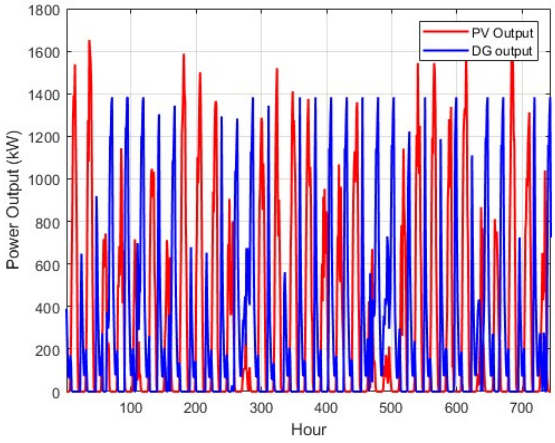

Figure 17. Scenario 3: PV and DG output in December (summer).

To further analyze daily operational patterns, a three-day sample is picked and analyzed, focusing on the trend between solar PV generation, and BESS charging and discharging, as well as the generator intervention in serving the load demand. As shown in Figure 18, during the winter season, the system successfully meets the load demand by over 99% due to the timely DG intervention. Moreover, a similar trend is realized for the summer season, as shown in Figure 19. Nonetheless, despite achieving high reliability, this configuration results in a slightly higher LCOE compared to the 1st and 2nd scenarios, which is estimated at \$0.026/kWh. The optimized component capacities obtained from the simulation are 2158.0542 kW for the solar PV system, 653 units for the BESS, and 2416.18 kW for the DG size. Although the diesel generators are present on Unguja Island, the high LCOE is primarily caused by the high operational costs and high fuel prices that keep escalating over the years, as Unguja Island relies on imported fuel from other countries. Over the project lifetime, the total fuel expenditure is estimated at \$830,288, with associated CO_2 emissions amounting to approximately 2225 tons, which raises concerns about the long-term environmental suitability of the configuration.

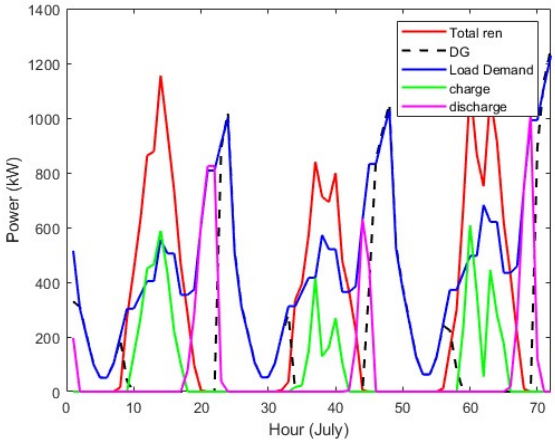

Figure 18. PV, DG, load & BESS profiles for 3 representative days in July (winter).

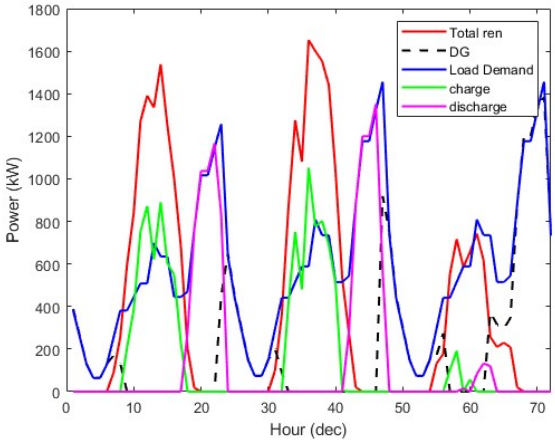

Figure 19. PV, DG, load & BESS profiles for 3 representative days in December (summer).

3.4. Sensitivity analysis

To assess how changes in operational and other lifecycle-related expenditures impact the levelized cost of electricity generation, a sensitivity analysis is performed across all microgrid configurations. This specific assessment focused on the variation in replacement costs and operation and maintenance (O&M) costs, which are known to play a pivotal role in long-term system economics. A cost reduction factor ranging from 0.5 to 1.4, equivalent to a 50% decrease and a 40% increase, relative to baseline costs, is applied. These margins are selected to reflect possible future cost shifts influenced by technological advancements, economic trends, or disruptions in global supply chains.

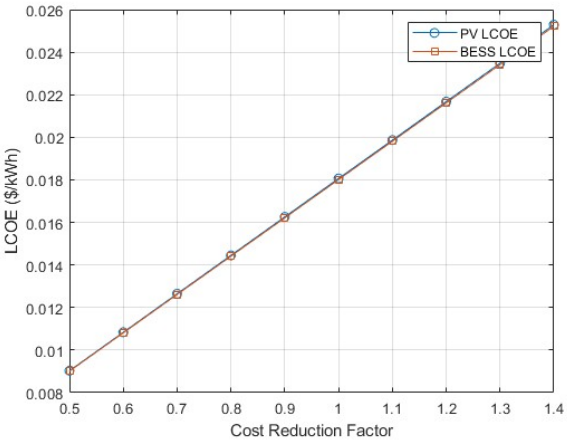

Figure 20. Sensitivity analysis for Scenario 1: examining the influence of PV & BESS life-cycle costs on LCOE.

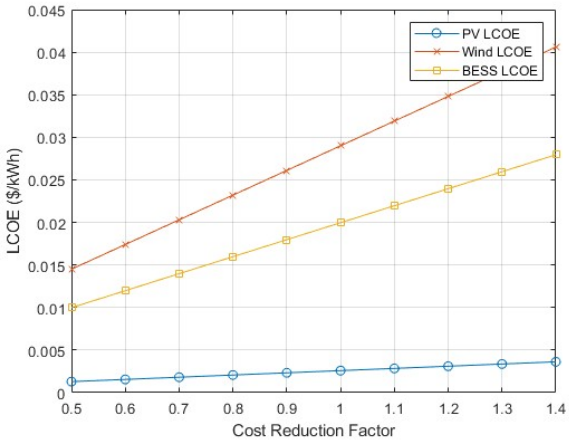

Figure 21. Sensitivity analysis for Scenario 2: examining the influence of PV, wind & BESS life-cycle costs on LCOE.

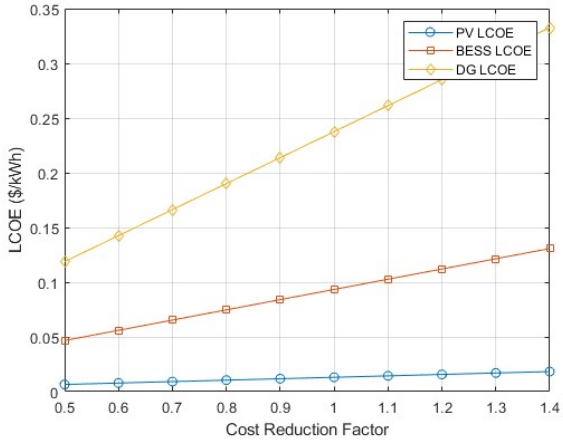

Figure 22. Sensitivity analysis for Scenario 3: examining the influence of PV, BESS & DG life-cycle costs on LCOE.

Figure 20 presents the sensitivity analysis results for Scenario 1, which operates exclusively on solar PV coupled with battery energy storage (BESS). The figure signifies that both PV and BESS contribute proportionately to the system's overall economic performance when replacement and O&M costs are adjusted. In this configuration, a large capacity of solar PV is required to meet daytime demand, leading to considerable O&M obligations, even though PV systems typically do not require full replacement during the project lifetime. Therefore, the PV contribution to LCOE is primarily shaped by long-term operational upkeep. On the other hand, the BESS plays an important role in balancing energy by storing excess generated energy and supplying energy during periods of low or no irradiation. Unlike PV, the BESS component incurs both high maintenance requirements and periodic replacements, typically every 10 years. As a result, any reduction in the operation and replacement costs of the BESS would have a significant impact on lowering the LCOE and enhancing the viability of this microgrid configuration.

Figure 21 illustrates the sensitivity results for Scenario 2, which consist of PV, wind energy, and BESS. Among these components, the wind system exhibits the most significant influence on the Levelized Cost of Energy (LCOE). As the cost reduction factor increases, the LCOE attributed to wind rises sharply, proving its dominant share in the overall system economics. Ongoing efforts to enhance the operational lifetime of major wind components and conduct condition-based maintenance using remote monitoring can considerably reduce long-term operation costs.

In addition to wind, the BESS component exerts a moderate influence on the LCOE. While less steep than wind, the upward trend in BESS LCOE across the cost reduction range indicates that its replacement frequency and maintenance overhead are non-negligible. Since the battery system plays a vital role in compensating for the intermittency of both PV and wind, its cost behavior has a meaningful impact on system viability. Reducing the cost of battery replacements, enhancing storage efficiency, and improving degradation control strategies would further enhance the affordability of this configuration. Furthermore, the contribution of the solar PV system to LCOE is relatively lower in this case. This is largely due to the reduction in the required capacity of the PV system as a result of hybrid wind energy inclusion, which helps offset solar variability, especially during periods of low irradiance.

Figure 22 presents the sensitivity analysis for Scenario 3, which comprises PV, BESS, and a diesel

generator (DG). Despite no initial capital investment for the generators due to the presence of existing DG on the Island, the system's LCOE is highly sensitive to the existence of the diesel generators. This is mainly impacted by the fuel consumption, as Unguja Island relies on fuel importation from other countries, with the fuel price escalating over the years. Furthermore, the inactive mode of the DG for over a decade would likely result in considerable maintenance costs in reactivating them, which can add significantly to the overall energy cost. Although the influence of BESS in this configuration is less obvious than that of the diesel generator, the battery plays a vital role in minimizing the dependence on the diesel generator. Hence, lowering the operational costs of BESS is effective in improving the feasibility of this configuration.

4. Conclusions

For many years, Unguja Island has been relying on electricity importation from the Tanzania mainland, which has significantly compromised its energy security due to the vulnerability of the submarine cables and the instability in the mainland's power infrastructures. The continuous expansion of tourism and other economic sectors on the island has necessitated the presence of a reliable and sustainable electricity supply on the island. In response, this study explores the feasibility of deploying hybrid standalone microgrids to cater to the electricity demand for a village in the northern region of Unguja Island.

The key conclusions drawn from this research are summarized below:

1. The study employed the Particle Swarm Optimizer (PSO) algorithm to evaluate the performance of three standalone microgrid configurations, optimized to meet the electricity demand for a village in northern Unguja Island, while also satisfying the reliability metrics. The three introduced case scenarios are:
    - Scenario 1: PV/BESS,
    - Scenario 2: PV/Wind/BESS,
    - Scenario 3: PV/BESS/DG.
2. The objective was to minimize the Levelized Cost of Energy (LCOE) throughout the project lifetime while ensuring the Loss of Power Supply Reliability (LPSP) to be under 0.04.
3. Scenario 2 achieved the most cost-effective performance with an LCOE of \$0.014/kWh, which is approximately 13.6% lower than Scenario 1 (\$0.0162/kWh) and 46.2% lower than Scenario 3 (\$0.026/kWh).
4. Scenario 3 demonstrated the highest reliability, achieving 99.99% load coverage. This was made possible by the integration of the diesel generator, which operated during periods when both PV output and battery reserves were insufficient. However, this configuration had the highest LCOE due to the higher cost of operations attributed to volatile fuel costs and periodic maintenance costs.
5. Furthermore, sensitivity analysis pointed out that BESS costs (particularly O&M and replacement costs) significantly influence LCOE across all scenarios. However, the costs of the wind system were the most critical in Scenario 2, while the operational costs of the diesel generator dominated Scenario 3. Hence, reductions in cost parameters can considerably improve the economic feasibility of employing these microgrids.

Despite promising results, the study has several limitations. The analysis entailed static meteorological data (solar irradiance, wind speed, and ambient temperature) for the year 2023, which may not represent the long-term climatic variations of the project lifetime. Moreover, the sensitivity analysis focused only on lifecycle cost variations and did not account for future changes in load demand. Optimization was carried out using a single-objective PSO approach aimed at minimizing LCOE under a reliability constraint LPSP < 0.04, which may have limited the exploration of trade-offs among multiple objectives. Furthermore, the infeasible solutions in the PSO approach were penalized to discourage the infeasible candidates; however, their exact frequency during the simulation was not tracked.

4.1. Future research directions

- Comparative studies will be conducted using other metaheuristic algorithms, such as Genetic Algorithm (GA) and Multiobjective PSO (MOPSO), to validate the robustness of the results.
- Dynamic demand growth modeling will be incorporated to assess the scalability of the proposed systems in future trends of energy consumption.
- Future studies will focus on the integration of electric vehicles as part of the energy management schemes; whereas instead of curtailing the excess energy, it can be directed to the electric vehicles.

This study demonstrates the technical and economic potential of optimized standalone hybrid microgrids to improve energy independence in remote communities. The study provides a baseline for future system planning, policy design, and investment prioritization in the Unguja Island energy sector.

Use of AI tools

We, the authors, declare that we have not used Artificial Intelligence (AI) tools in the creation of this article.

Acknowledgments

I would like to extend my gratitude to the the Japan International Cooperation Agency (JICA) for giving me a scholarship to do my Master's Degree in Japan.

Conflicts of interest

There is no conflict of interest.

Author contributions

Author Fathia Jombi Kheir: Conception and design of study, Data acquisition and Analysis, Programming, Visualization, and Writing of Original Draft. Author Soichiro Ueda: Review of concepts and design of the study. Author Takuma Ishibashi: Conceptualization. Author Mitsunaga Kinjo: Article Review. Author Issoufou Tahirou Halidou: Technical Revision and Interpretation. Author Masahiro Furukakoi: Writing Review and Interpretation. Author Tomonobu Senjyu: Concept Design & Review, Editing and Supervision.

References

1. Das BK, Alotaibi MA, Das P, et al. (2021) Feasibility and techno-economic analysis of stand-alone and grid-connected PV/Wind/Diesel/Batt hybrid energy system: A case study. *Energy Strateg Rev* 37: 100673. https://doi.org/10.1016/j.esr.2021.100673
2. Mission 300 Connecting 300 Million People to Electricity. Available from: https://mission300africa.org/energysummit/wp-content/uploads/2024/12/mission300.pdf.
3. Surroop D, Raghoo P (2018) Renewable energy to improve energy situation in African island states. *Renewable Sustainable Energy Rev* 88: 176–183. https://doi.org/10.1016/j.rser.2018.02.024
4. Santos SF, Fitiwi DZ, Shafie-khah M, et al. (2017) Introduction to renewable energy systems, In: Ozan Erdinç (ed) *Optimization in Renewable Energy Systems*. Academic Press, Cambridge, MA, 1–26. https://doi.org/10.1016/B978-0-08-101041-9.00001-6
5. Bull SR (2001) Renewable energy today and tomorrow. *P IEEE* 89: 1216–1226. https://doi.org/10.1109/5.940290
6. Chebabhi A, Tegani I, Benhamadouche AD, et al. (2023) Optimal design and sizing of renewable energies in microgrids based on financial considerations: A case study of Biskra, Algeria. *Energ Convers Manage* 291: 117270. https://doi.org/10.1016/j.enconman.2023.117270
7. Zibi, Towards Zanzibar Energy Security: The Next Steps in Zanzibar's Power Evolution, 2025. Available from: https://zibi.co.tz/towards-zanzibar-energy-security/.
8. Revolutionary Government of Zanzibar (2024) *The Zanzibar Energy Sector Transformation Project: Project Procurement Strategy for Development*. Available from: https://documents1.worldbank.org/curated/en/099151003232326098/pdf/P1695610c5ee9f0fd08ff-40e728ae3e8295.pdf.
9. World Bank Group (2017) Utility-scale Solar PV and Battery Energy storage System (BESS) for Zanzibar Archipelago Renewable Energy Solution. Available from: https://www.esmap.org/sites/default/files/ESP/23_Tanzania_zanzibar.pdf.
10. Westphal I (2024) The effects of reducing renewable power intermittency through portfolio diversification. *Renew Sustain Energy Rev* 197: 114415. https://doi.org/10.1016/j.rser.2024.114415
11. El-Sattar HA, Hassan MH, Vera D, et al. (2024) Maximizing hybrid microgrid system performance: A comparative analysis and optimization using a gradient pelican algorithm. *Renewable Energy* 227: 120480. https://doi.org/10.1016/j.renene.2024.120480
12. Chen B, Xiong R, Li H, et al. (2019) Pathways for sustainable energy transition. *J Cleaner Prod* 228: 1564–1571. https://doi.org/10.1016/j.jclepro.2019.04.372
13. Anand P, Kamboj VK, Rizwan M (2024) Optimal sizing of hybrid energy system using an improved gazelle optimization algorithm. *Electr Eng* 107: 7263–7296. https://doi.org/10.1007/s00202-024-02892-w
14. Sinha S, Chandel SS (2014) Review of software tools for hybrid renewable energy systems. *Renewable Sustainable Energy Rev* 32: 192–205. https://doi.org/10.1016/j.rser.2014.01.035

15. Fodhil F, Hamidat A, Nadjemi O (2019) Potential, optimization and sensitivity analysis of photovoltaic-diesel-battery hybrid energy system for rural electrification in Algeria. *Energy* 169: 613–624. https://doi.org/10.1016/j.energy.2018.12.049

16. Tudu B, Majumder S, Mandal KK, et al. (2011) Comparative performance study of genetic algorithm and particle swarm optimization applied on off-grid renewable hybrid energy system. *Swarm Evol Memetic Comput* 2: 151–158. https://doi.org/10.1007/978-3-642-27172-4_19

17. Lamedica R, Santini E, Ruvio A, et al. (2018) A MILP methodology to optimize sizing of PV-Wind renewable energy systems. *Energy* 165: 385–398. https://doi.org/10.1016/j.energy.2018.09.087

18. Zhao B, Zhang X, Li P, et al. (2014) Optimal sizing, operating strategy and operational experience of a stand-alone microgrid on Dongfushan Island. *Appl Energy* 113: 1656–1666. https://doi.org/10.1016/j.apenergy.2013.09.015

19. Bukar AL, Tan CW, Lau KY (2019) Optimal sizing of an autonomous photovoltaic/wind/battery/diesel generator microgrid using the grasshopper optimization algorithm. *Sol Energy* 88: 685–696. https://doi.org/10.1016/j.solener.2019.06.050

20. Abusaq M, Zohdy MA (2024) Optimal sizing of solar off-grid microgrid using modified firefly algorithm. *Int J Sci Eng Sci* 8: 8–16. Available from: https://ijses.com/wp-content/uploads/2024/08/30-IJSES-V8N8.pdf.

21. NASA. POWER Data Access Viewer. Available from: https://power.larc.nasa.gov/data-access-viewer/.

22. Irshad AS, Kargar N, Elkholy MH, et al. (2024) Techno-economic evaluation and comparison of the optimal PV/Wind and grid hybrid system with horizontal and vertical axis wind turbines. *Energy Convers Manage: X* 23: 100638. https://doi.org/10.1016/j.ecmx.2024.100638

23. Halidou IT, Elkholy MH, Senjyu T, et al. (2025) Optimal microgrid planning for electricity security in Niamey: A strategic response to sudden supply disruptions from neighboring sources. *Energy Convers Manage* 326: 119529. https://doi.org/10.1016/j.enconman.2025.119529

24. Diab AAZ, Sultan HM, Mohamed IS, et al. (2019) Application of different optimization algorithms for optimal sizing of PV/wind/diesel/battery storage stand-alone hybrid microgrid. *IEEE Access* 7: 119223–119245. https://doi.org/10.1109/ACCESS.2019.2936656

25. Hamilton JM, Negnevitsky M, Wang X, et al. (2017) Utilization and optimization of diesel generation for maximum renewable energy integration, In: Islam F, Mamun K, Amanullah M (eds) *Smart Energy Grid Design for Island Countries*, Green Energy and Technology. Springer, Cham, 1: 21–70. https://doi.org/10.1007/978-3-319-50197-0_2

26. Jafari A, Khalili T, Ganjehlou HG, et al. (2020) Optimal integration of renewable energy sources, diesel generators, and demand response program from pollution, financial, and reliability viewpoints: A multi-objective approach. *J Cleaner Prod* 247: 119100. https://doi.org/10.1016/j.jclepro.2019.119100

27. Ramesh M, Saini RP (2020) Effect of different batteries and diesel generator on the performance of a stand-alone hybrid renewable energy system. *Energy Sources, Part A* 46: 7983–8005. https://doi.org/10.1080/15567036.2020.1763520

28. Ouyang X, Lin B (2014) Levelized cost of electricity (LCOE) of renewable energies and required subsidies in China. *Energy Policy* 70: 64–73. https://doi.org/10.1016/j.enpol.2014.03.030

29. Bruck M, Sandborn P, Goudarzi N (2018) A Levelized Cost of Energy (LCOE) model for wind farms that include Power Purchase Agreements (PPAs). *Renewable Energy* 122: 131–139. https://doi.org/10.1016/j.renene.2017.12.100

30. Tabak A, Kayabasi E, Guneser MT, et al. (2022) Grey wolf optimization for optimum sizing and controlling of a PV/WT/BM hybrid energy system considering TNPC, LPSP, and LCOE concepts. *Energy Sources, Part A* 44: 1508–1528. https://doi.org/10.1080/15567036.2019.1668880

31. Agyekum EB, Nutakor C (2020) Feasibility study and economic analysis of stand-alone hybrid energy system for southern Ghana. *Sustain Energy Technol Assess* 39: 100695. https://doi.org/10.1016/j.seta.2020.100695

32. Chauhan A, Saini RP (2016) Techno-economic feasibility study on integrated renewable energy system for an isolated community of India. *Renewable Sustainable Energy Rev* 59: 388–405. https://doi.org/10.1016/j.rser.2015.12.290

33. Ghosh A, Norton B (2019) Optimization of PV powered SPD switchable glazing to minimise probability of loss of power supply. *Renewable Energy* 131: 993–1001. https://doi.org/10.1016/j.renene.2018.07.115

34. Ayop R, Isa NM, Tan CW (2018) Components sizing of photovoltaic stand-alone system based on loss of power supply probability. *Renewable Sustainable Energy Rev* 81: 2731–2743. https://doi.org/10.1016/j.rser.2017.06.079

35. Phommixay S, Doumbia ML, Lupien St-Pierre D (2020) Review on the cost optimization of microgrids via particle swarm optimization. *Int J Energy Environ Eng* 11: 73–89. https://doi.org/10.1007/s40095-019-00332-1

36. Phan-Van L, Takano H, Duc TN (2023) A comparison of different metaheuristic optimization algorithms on hydrogen storage-based microgrid sizing. *Energy Rep* 9: 542–549. https://doi.org/10.1016/j.egyr.2023.05.152

37. Flores-Livas JA, Boeri L, Sanna A, et al. (2020) A perspective on conventional high-temperature superconductors at high pressure: Methods and materials. *Phys Rep* 856: 1–78. https://doi.org/10.1016/j.physrep.2020.02.003

38. Jain M, Saihjpal V, Singh N, et al. (2022) An overview of variants and advancements of PSO algorithm. *Appl Sci* 12: 8392. https://doi.org/10.3390/app12178392

39. Nuzulack Dausen (2024) Tanzania central bank holds key rate, sees strong economic growth. *Reuters* Available from: https://www.reuters.com/markets/tanzania-central-bank-holds-key-rate-sees-strong-economic--growth-2024-07-04/.

40. Li Z, Ma T (2022) Theoretic efficiency limit and design criteria of solar photovoltaics with high visual perceptibility. *Appl Energy* 324: 119761. https://doi.org/10.1016/j.apenergy.2022.119761

41. Halidou IT, Howlader HOR, Gamil MM, et al. (2023) Optimal power scheduling and techno-economic analysis of a residential microgrid for a remotely located area: a case study for the Sahara Desert of Niger. *Energies* 16: 3741. https://doi.org/10.3390/en16083471

42. Larsson P, Börjesson P. Cost models for battery energy storage systems. Bachelor of Science Thesis, KTH School of Industrial Engineering and Management, Stockholm, 2018. Available from: https://www.diva-portal.org/smash/get/diva2:1254196/FULLTEXT01.pdf.

43. Oliveira WS, Fernandes AJ (2013). Investment analysis for wind energy projects. *Revista Brasileira de Energia* 19: 239–285. Available from: https://sbpe.org.br/index.php/rbe/article/download/314/295/.

44. Stehly T, Duffy P, Hernando DM (2024) Cost of Wind Energy Review: 2024 Edition. *National Renewable Energy Laboratory.* Available from: https://docs.nrel.gov/docs/fy25osti/91775.pdf.

45. Longe OM, Rao N, Omowole F, et al. (2017) A case study on off-grid microgrid for universal electricity access in the Eastern Cape of South Africa. *Int J Energy Eng* 7: 55–63. Available from: https://pure.iiasa.ac.at/id/eprint/14777/1/10.5923.j.ijee.20170702.03.pdf.

AIMS Press